Long-range interaction of copper adatoms and copper dimers on Ag(111)

2005 New J. Phys. 7 139

(http://iopscience.iop.org/1367-2630/7/1/139)

New Journal of Physics
The open-access journal for physics

Long-range interaction of copper adatoms and copper dimers on Ag(1 1 1)

Karina Morgenstern[1,2,3] **and Karl-Heinz Rieder**[2]

[1] Institut für Festkörperphysik, Universität Hannover, Appelstr. 2, D-30167 Hannover, Germany
[2] Institut für Experimentalphysik, FB Physik, Freie Universität Berlin, Arnimallee 14, D-14195 Berlin, Germany
E-mail: morgenstern@fkp.uni-hannover.de

New Journal of Physics **7** (2005) 139
Received 11 February 2005
Published 2 June 2005
Online at http://www.njp.org/
doi:10.1088/1367-2630/7/1/139

Abstract. Formation and motion of copper adatoms and addimers on Ag(1 1 1) are investigated with low-temperature scanning tunnelling microscopy between 6 and 25 K. Adatoms move between fcc and hcp sites with a strong preference for the fcc site. Adatom motion and dimer rotation change due to the presence of other adatoms or dimers. Furthermore, rotating dimers influence other rotating dimers. These changes are attributed to changes in the diffusion or rotation potential, which are mediated by the electrons in the two-dimensional surface state band.

Contents

1. Introduction

A comprehensive picture that connects diffusional properties on the atomic level with macroscopic patterns that develop during growth requires deep insight into motion and aggregation of adparticles starting from monomers. Thus, numerous experiments and accurate

[3] Author to whom any correspondence should be addressed.

PII: S1367-2630(05)94645-4

theoretical calculations have addressed the diffusion of single adatoms [1]–[7]. Fewer studies have dealt with the properties of dimers [8]–[10] or even larger adparticles [11], although theory suggests dimer diffusion to be important, e.g. for mass transport [12] and for step bunching instabilities during growth [13].

Important information on the processes of diffusion on metal surfaces has been gathered with field ion microscopes [5]. An inherent information gap left by this valuable method is starting to be filled by application of scanning tunnelling microscopy (STM). Some experimental difficulties, however, still hamper this development and the number of direct STM studies on adatom migration is therefore limited [14]–[18]. The main problem is the inadequacy between the scanning speed of STM imaging and the rate of diffusional motion [10] (for a discussion of this problem, see [19]). To circumvent this problem, conclusions about atomistic motion have been drawn from the observation of larger and thus slower adparticles [11] revealing that a complete characterization of the diffusion process of adparticles is much more complicated than that for single adatoms. Theory has shown that this is already true for the case of dimers [20].

Concerning the interaction between adparticles, there are different interactions depending on adparticle distance. At small separation, direct electronic interactions prevail leading to localized chemical bonds [21], i.e. to dimers or larger adparticles. At larger separations, adsorbate interactions can be mediated either by electrostatic (dipole–dipole) and elastic (deformation of substrate lattice) fields, which decay with separation d as $1/d^3$, or via oscillatory Friedel-type interactions decaying asymptotically as $\sin(2q_F d)/d^2$ in the case of a filled surface band and as $\cos(2q_F d)/d^5$ otherwise [22], with q_F the in-plane Fermi vector. In the case of an occupied surface state, each adparticle induces scattering of the electrons and causes spatial oscillations in the surface band density of states (DOS). As the binding energy of an adparticle depends on electron density, the interference between such DOS variations produce a Friedel-type adparticle–adparticle interaction, whose interaction energy also oscillates with the mutual adparticle separation d. In the limit of large separation [23]:

$$\Delta E_{\text{pair}} \approx -\epsilon_F \left(\frac{2\sin\,\delta_F}{\pi}\right)^2 \frac{\sin(2q_F d + 2\delta_F)}{(q_F d)^2} \tag{1}$$

with the in-surface Fermi wave vector $q_F = \sqrt{2m_{\text{eff}}\epsilon_F}$ and the phase shift δ_F. This asymptotic expression has been shown to be accurate down to distances of $\lambda_F/2$ [23], with λ_F the Fermi wavelength. Bogicevic *et al* [22] calculated for copper adatoms on Cu(1 1 1) that indirect interactions lead to a binding energy variation of about 46 meV. Experimentally, the repulsion barrier was estimated to lie between 10 and 14 meV [24]. STM measurements revealed strong effects on adsorbate arrangement due to these oscillatory interactions [15, 16, 25]. The surface state electrons thus influence the adatom motion at low temperature by modifying the diffusion potential in oscillatory form.

In a recent letter, we sketched results for adatom and dimer motion and interaction in the hetero-epitaxial case of copper on Ag(1 1 1) [18]. We showed that in this system also the adatom motion is influenced by the surface electron oscillations around other adatoms. An even stronger long-range oscillation was found for the interaction of adatoms with dimers.

In this paper, we present additional data on the adatom motion, particularly the diffusion between hcp and fcc sites. Furthermore, temperature-dependent data are presented about the influence of adatoms on dimer rotation. Finally, we show the influence of dimer orientation on rotation of other dimers.

2. Experimental procedure

The experiments are performed in ultrahigh vacuum with a low-temperature STM which operates at temperatures between 6 and 300 K [26]. The single crystalline Ag(1 1 1) surface is cleaned by sputtering and annealing cycles. Copper is deposited from a home-built evaporator on to the cold surface within the shields of the STM at 7 K. Measurements are performed between 6 and 25 K. Special care is taken that imaging does not influence the measurements [27].

3. Results and discussion

Figure 1(a) shows the surface directly after deposition. Three types of protrusions are discernible in figure 1(a); most frequently, circular protrusions with an apparent height of 40 pm at 100 mV and 85 pm at 210 mV (figure 1(b)), and a FWHM of 0.42 nm (with the sharpest tips). These are adatoms. The ellipsoidal protrusions with an apparent height of 65 pm at 100 mV and 137 pm at 210 mV (figure 1(b)) and a FWHM of 0.62 and 0.48 nm along its long and short axis, respectively, are dimers as verified by direct observation of dimer formation. Dimer formation (figure 2) is observed above 19 K on the timescale of the experiment and increases the number of dimers.[4] In addition, we observe bright spots with more than twice the apparent height (D_m in figure 1(a)), which disappear by raising the temperature to 8.1 K (figure 1(c)). As Cu deposition reduces the mean value of impurities prior to deposition ($1/(16.5\ \mathrm{nm})^2$) only slightly to $1/(15.8\ \mathrm{nm})^2$ on average, the bright spots with a density of $1/(15.3\ \mathrm{nm})^2$ cannot be related to copper atoms adsorbed on or near impurities. We attribute those tentatively to metastable dimers with a smaller in-plane atomic distance than regular dimers, which necessitates out of place displacement.

The distance distribution function (figure 1(d)) has a mean value of 9 and 16 nm for an image size of 18.75 nm $\times$ 18.75 nm (figure 1(d1)) and 34.9 nm $\times$ 34.9 nm (figure 1(d2)), respectively. In the distance distribution we count all distances measurable between atoms on the STM image, regardless of whether or not there is another atom on the direct path between them. The distance distribution is in accordance with a random deposition of adatoms. However, very small distances do not exist: for more than 10 000 measured distances, only once a distance of 0.5 nm was observed, all other distances are larger than 0.6 nm. Thus a short-range repulsion already influences the adsorption of the adatoms.

We followed the diffusion of adatoms and dimers for temperatures between 6 and 25 K by recording images at regular time intervals between 45 and 200 s. The upper temperature limit is imposed by the frequency of position changes as compared to the scanning speed. At elevated temperatures we observe position changes of the adatoms during scanning and dimers that appear as trimers (figure 3(a)). The steep Arrhenius-like increase in the not-identifiable dimer positions (figure 3(b)) suggests that we have reached the experimental temperature limit. Enhancing the scanning speed of the STM will only slightly rise the highest possible temperature. More importantly, at 24 K adatoms are lost to pre-existing step edges or due to adparticle formation, such that no adatoms are left on the terrace. For Cu/Cu(1 1 1) the same problem exists at a slightly lower temperature of 22 K [24].

[4] At 8 K we observe only two adatom motions for 42 832 recorded events at time intervals of 200 s. For dimer diffusion we observe a single event at 24.3 K for 3330 recorded events at time intervals of 100 s. This means that a single adatom moves on average once within 50 days at 8 K and a dimer moves out of the cell once within 4 days at 24.3 K, and thus we consider these motions as not yet activated at the respective temperatures.

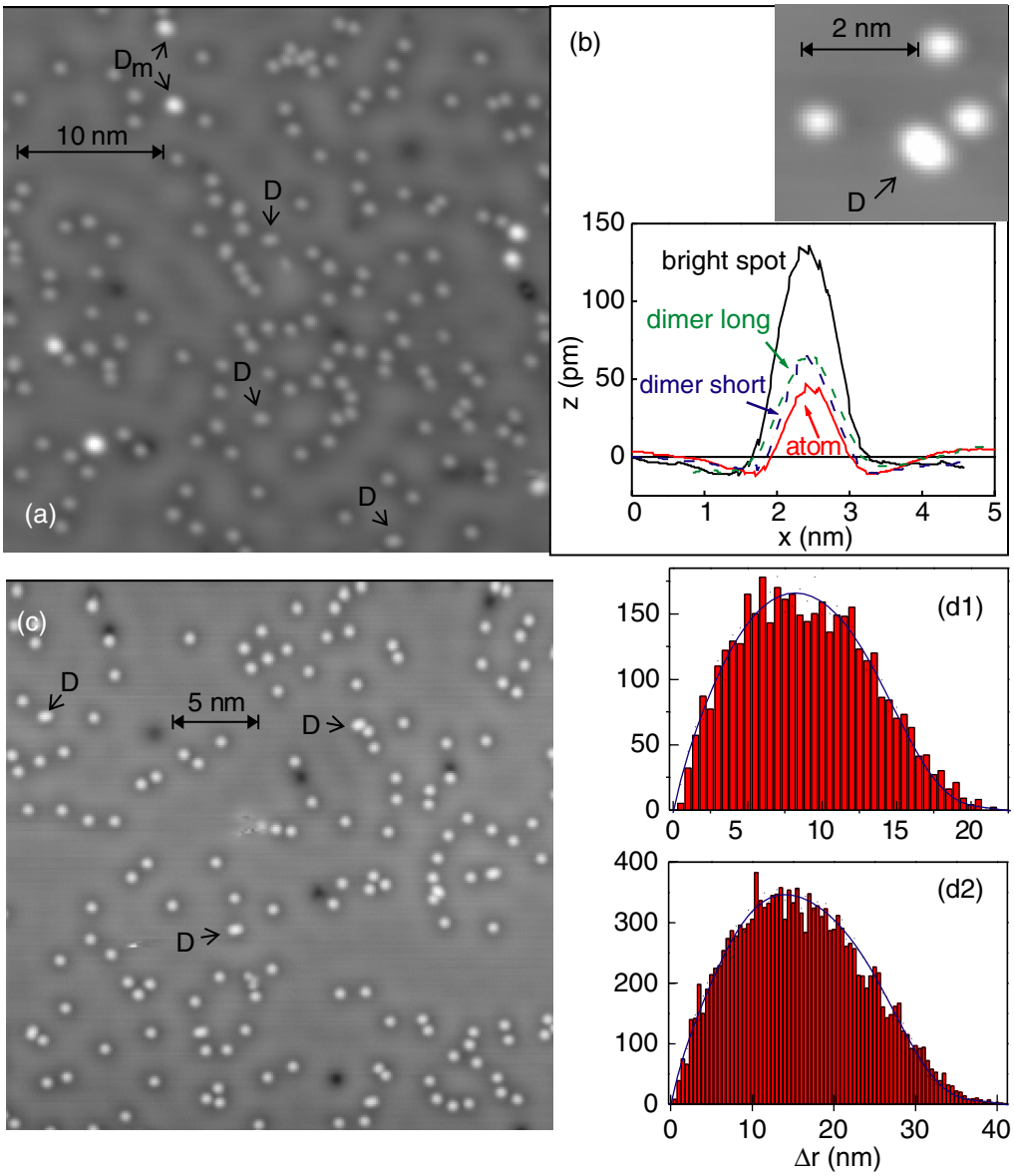

Figure 1. Deposition of adatoms at low temperature (7 K). (a) Large-scale STM image of Cu adatoms (circular protrusion) and Cu dimers (ellipsoidal protrusions, some marked with D) and some bright spots (see text, marked D_m) on Ag(1 1 1) directly after deposition; coverage of approximately 1.5% ML (5.6 K, $U_t = 99$ mV, $I_t = 0.65$ nA). (b) Line scans through maximum of protrusion of adatom, dimer (in two perpendicular directions), and bright spot; inset shows adatoms and dimer at higher resolution (7 K, 210 mV, 0.82 nA). (c) STM image of Cu adatoms (circular protrusion) and Cu dimers (ellipsoidal protrusions, some marked with D) on Ag(1 1 1); same deposition as in (a), but in a different part of the surface and at a higher measurement temperature (8.1 K, 210 mV, 0.47 nA). (d) Histogram of distances Δr between adatoms directly after deposition for 18.8 and 34.9 nm image size, respectively; the solid line is the expected random distribution for this image size and adatom density.

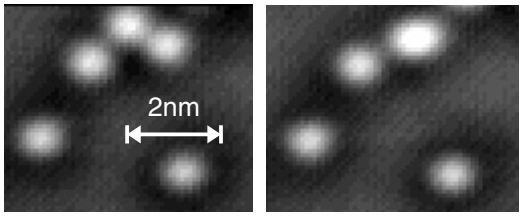

Figure 2. Dimer formation: $\Delta t = 100$ s, 20 K, 203 mV and 0.43 nA.

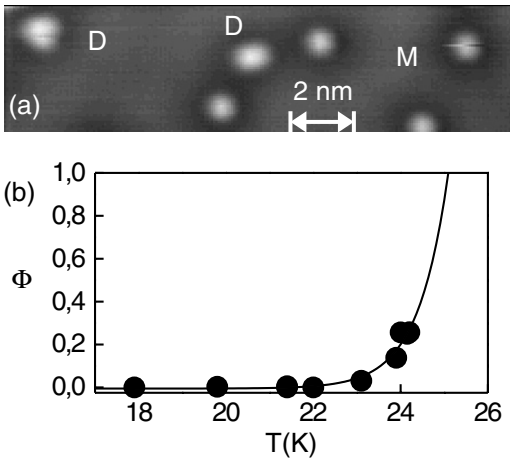

Figure 3. Experimental limits: (a) rotating dimer (D) in upper-left corner looks like a trimer and monomer (M) moves during scan (23.7 K, 200 mV, 0.4 nA) and (b) percentage of the not-identifiable dimer positions Φ versus temperature T, the line is an exponential fit.

Figure 4 shows snapshots of two movies that record motion at two different temperatures over 8 h. Movies are available at [28]. The dark impurity in snapshot (a) is immobile at 21 K and is used as a reference point to compensate for thermal drift. In snapshot (b) a protrusion at the step in the lower-left corner serves this aim. The adatom motion is random and increases with temperature. Two adatoms as followed in the movie (see [28]) are marked in figure 4 for clearer impression. From the temperature dependence of the adatom diffusivity, we determined an activation energy of (65 ± 9) meV for adatom motion [18].

On fcc surfaces, monomers may occupy the fcc as well as the metastable hcp site (figure 5(a)) and thus move between these two non-equivalent sites. In the experiment, the adatoms move, however, predominately by lattice constant distances (figure 5(b)) indicating hops between equivalent sites. At this temperature, the hopping rate is so small, i.e., the average residence time of an atom on a certain site is so large, that only single hops are observed and all hops are expected to be seen. In rare cases, intermediate sites are occupied (figure 5(b) at ∼19 000 s). From the sites visited during the 8 h movie of figure 4(a) as recorded in figure 5(c) it is possible to construct the atomic lattice. As shown for two examples, each adatom visits the intermediate sites but rather seldom. In this particular movie (at 21 K), the hcp and fcc sites are occupied for 207 and 7274 times respectively. This allows one to estimate the energy difference between the two sites to be (5.5 ± 1.0) meV. For Cu diffusion on Cu(1 1 1) only jumps by entire lattice spacings were observed [15]–[17] and the site was identified to be the fcc site. In agreement, theory for

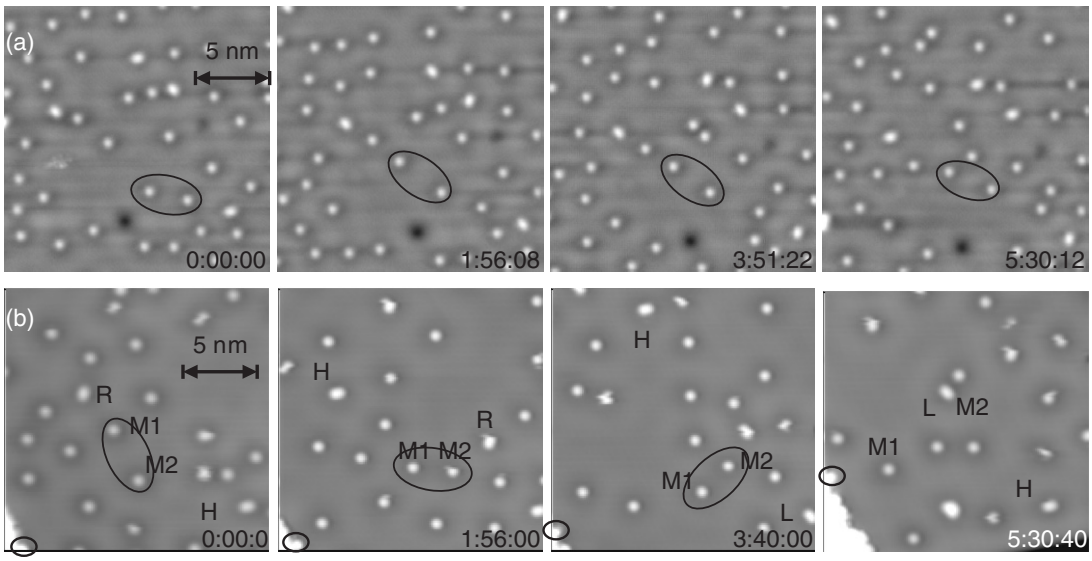

Figure 4. Snapshots of movies [28]: time lapse sequence of adatom and dimer motions. Letters R, L and H mark three possible dimer positions; the ellipse marks identical adatoms. (a) At 21 K (203 mV, 0.43 nA); $N = 262$ images; $\Delta t = 100$ s and total time covered by movie 1 $t_{\mathrm{tot}} = 7$ h 18 min. (b) At 24 K (200 mV, 0.4 nA); $N = 330$ images; $\Delta t = 80$ s and $t_{\mathrm{tot}} = 8$ h (see movie 2).

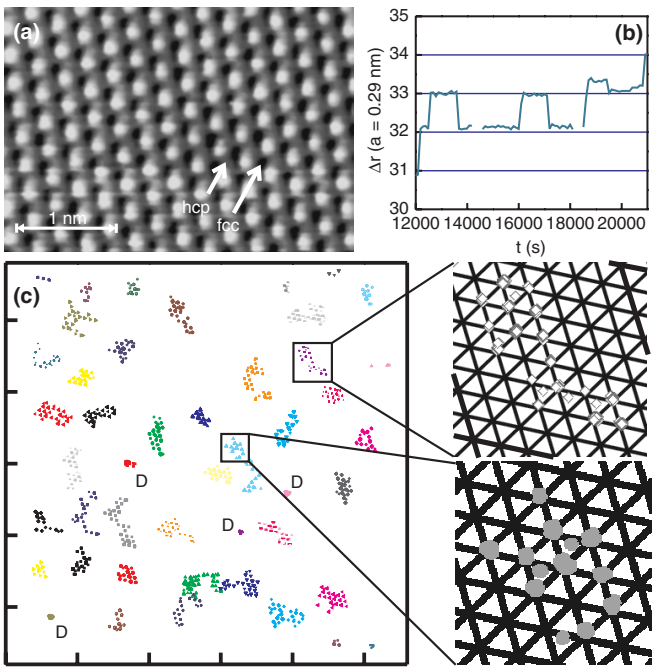

Figure 5. Adatom motion. (a) STM image pointing out fcc and hcp sites in an atomic resolution image; the height difference between these two sites is (15 ± 5) pm at a conductance of 1 nA and -1.24 V (cf [29]). (b) Position change of adatom in time; horizontal lines denote atomic surface distance. (c) Site map of adatoms in the movie in figure 4(a); each different symbol corresponds to a different adatom or dimer (D); zoom-in with atomic lattice constructed from the atom positions.

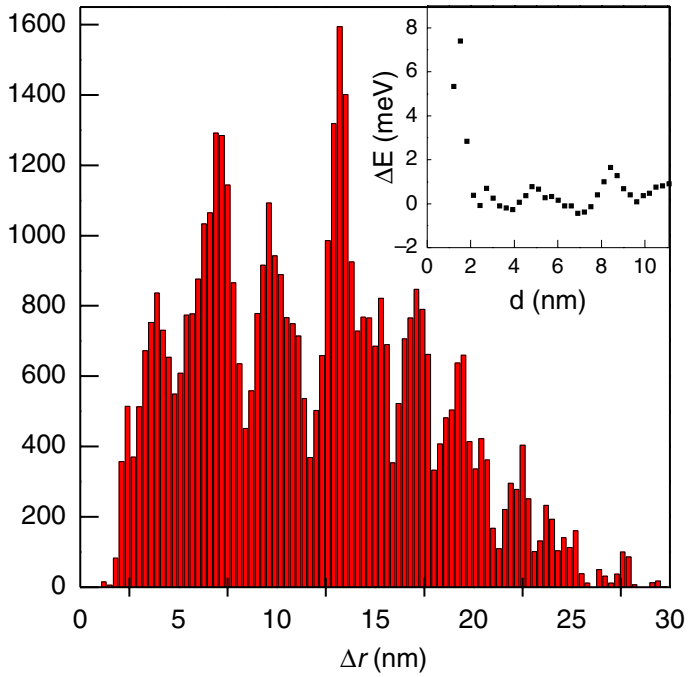

Figure 6. Oscillatory potential: distance distribution upon adatom motion between dimers at 21.5 K; inset shows change in diffusion energy derived from histogram as in [15].

Cu/Cu(1 1 1) finds the hcp site to be as unstable as the bridge site and therefore predicts diffusion to occur between fcc sites only [22]. To our knowledge, diffusion of Cu on Ag(1 1 1) has not been calculated with first principles.

In a distribution of distances between adatoms and dimers, strong oscillations are observed indicating that the adatom motion is influenced by the presence of dimers (figure 6). The first maximum, corresponding to the first potential minimum, is observed at 3.9 nm and seven minima are observed, up to a distance of 23.1 nm. The histogram in figure 6(b) shows that the dimers influence the adatom motion. The change in diffusion energy is, apart from the strong first repulsion, of the order of ± 1 meV (cf to Co/Ag(1 1 1) in [16]).

In the temperature range investigated, the dimer shows a rotation [18] in which it changes between three equivalent sites. These are marked with R (= right inclined), L (= left inclined) and H (= horizontal) in figures 4, 7 and 8. For isolated dimers, all three positions are observed equally often. In [18] we showed that the dimer rotation potential becomes asymmetric due to elastic deformation of the lattice, if a monomer is in close proximity. Also an influence at larger distances mediated by the surface state electrons was observed. In the examples shown in figure 7(a) only two positions, L and R, are observed for 28 consecutive images (2700 s), i.e. as long as the third adatom stays close by. As soon as the adatom has increased the distance to >1.7 nm all three orientations of the dimer are observed (see [28]). Thus, the long-range interaction leads to an asymmetry for individual dimers for distances of adatoms to dimers of up to several nanometres. In the example in figure 7(b), for a dimer surrounded by three adatoms, the rotation depends sensitively on the adatom distances (see [28]).

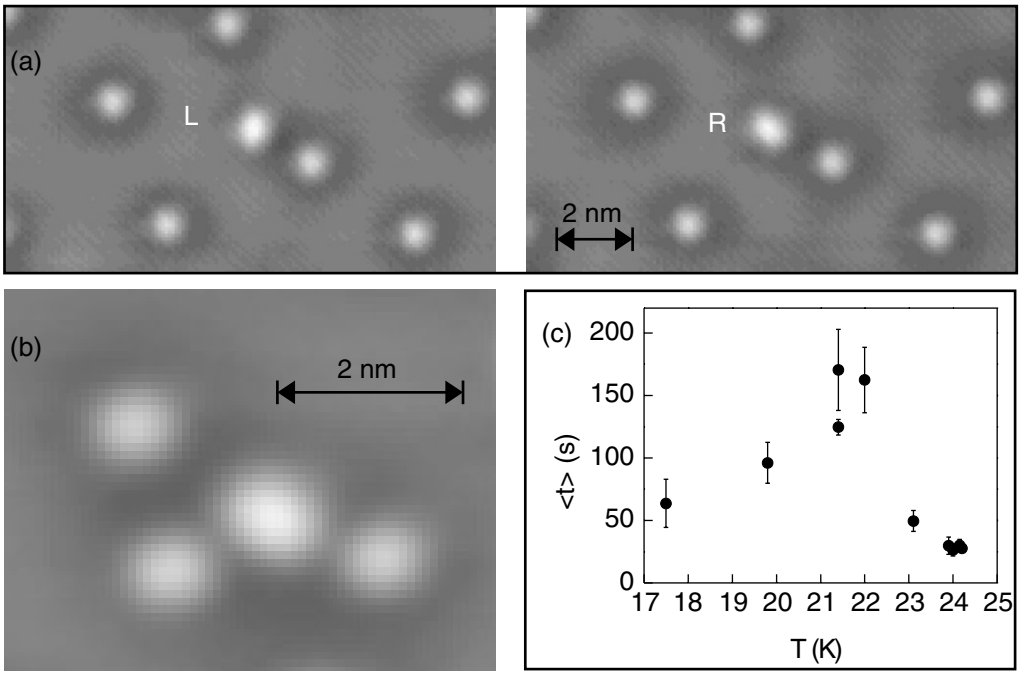

Figure 7. Influence of adatoms on dimer rotation ($\Delta t = 100$ s, 203 mV, 0.43 nA). (a) $T = 21$ K, closest distance from dimer to adatom $\Delta d = 1.68$ nm, dimer positions: LRRRRRLLLLLRRLRLLRRRLLLLLLLR. See movie 3 and movie 4. (b) $T = 17$ K, $\Delta d = 1.7$, 1.21 and 1.36 nm, consecutive dimer positions: RRRHHHLRRHLLLHLLLHLLH. See movie 5. (c) Average residence time $\langle t \rangle$ of a dimer in one of three equivalent positions during rotation versus temperature T.

Due to this influence, the average residence time of the dimer in one position before it changes to one of the other two increases with increasing temperature between 17.5 and 22 K (figure 7(c)); only above 23 K it decreases as expected for activated processes (Arrhenius behaviour). Thereby, the measured average time at high temperature represents an upper limit due to scanning speed limitations.

We can comprehend this non-Arrhenius behaviour by the onset of adatom diffusion, which is a prerequisite of an influence of the adatoms on to the dimer rotation. An increased diffusion leads to adatoms coming close enough to a dimer to stabilize a certain dimer position. The decrease at higher temperature is, however, an artifact of the decreasing adatom density with increasing temperature (see above). This interpretation is corroborated by a dependence of the average residence time of the dimer in one position before it changes to one of the other two positions on the (local) density of adatoms [18].

A noticeable influence of adatoms on dimer rotation requires a distance of less than 1.7 nm. For dimers we find a mutual influence on the rotation for even larger distances. Figure 8(a) shows an example of two dimers that have a distance of 3.7 nm. From the nine possible combinations of dimer orientations, the three most common ones, RL, RR and LR occur in 57% of all cases, while the three least frequent ones, HL, HR and RH only in 11% of the cases. Therein the orientation HL is never observed. In figure 8(b) for a distance of 2.4 nm the probabilities are 64% for RL, HL and HH and 11% for LL, LR and RH. None of the adatoms is close enough to explain

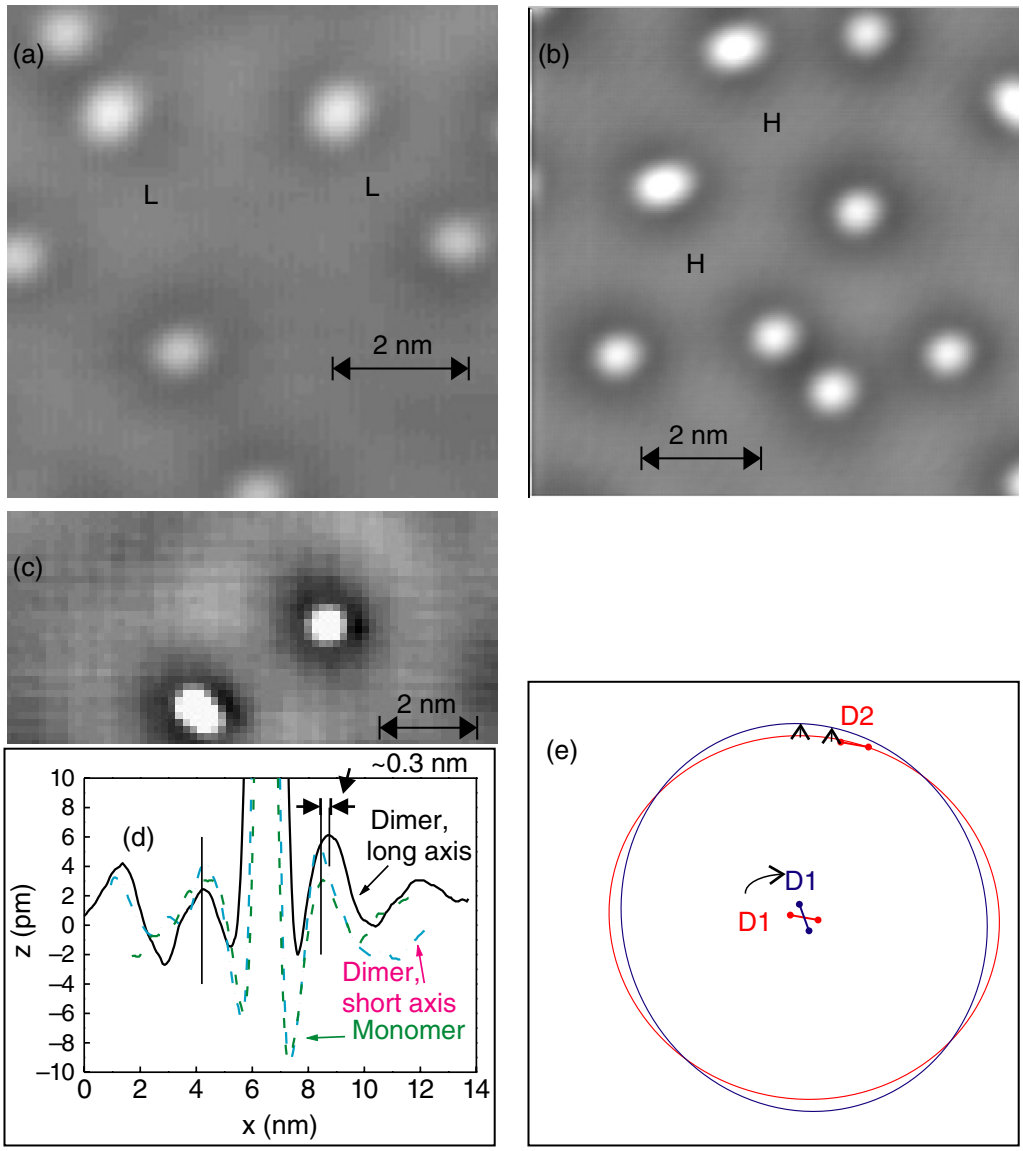

Figure 8. Mutual influence during dimer rotation ($\Delta t = 100$ s, 203 mV, 0.43 nA). (a) $T = 21$ K, distance between dimers $\Delta d = \lambda_F/2$. See movie 6. (b) $T = 21$ K, $\Delta d = 2.5$ nm. See movie 7. (c) Standing wave pattern around dimer as compared to monomer (44 mV, 0.22 nA). (d) Line scan through dimer and monomer including standing wave taken on two well-separated adparticles. (e) Sketch of change in the potential minimum upon dimer rotation (see text); the ellipses indicate the potential minimum due to dimer D1 in the two indicated orientations.

this behaviour by an adatom influence. Furthermore, in both cases the same orientation of an individual dimer is observed in the most frequent and the least frequent pair orientations. Thus, rotations of dimers with distances of up to at least $\lambda_F/2$ is not independent of each other.

This can be understood by realizing that the standing wave pattern around the ellipsoidal dimer is also slightly ellipsoidal (figure 8(c)) with an aspect ratio of 1.06. The smaller diameter is similar to the one around an isolated adatom (figure 8(d)). The larger diameter is the sum of the

atom distance plus the standing wave around an isolated atom. Thus, the potential maxima and minima around a rotating dimer shift on the order of half-a-lattice distance during dimer rotation, changing thereby the rotational potential of the neighbouring dimer. Consider, for example, the situation sketched in figure 8(e). In the initial position, dimer D1 is horizontal and dimer D2 at a distance of 3.7 nm lies with both atoms within the potential minimum. Now dimer D1 rotates clockwise. To regain the most favourable adsorption site, D2 would have to diffuse as indicated by the arrow. However, as long as the temperature is too low for dimer diffusion, it might get a more favourable adsorption site by rotation. Whether or not the new site is energetically favourable depends on the distance and relative orientation of the dimers to each other. We hope to induce theoretical effort into this direction through our results.

4. Conclusion

On the system Cu/Ag(1 1 1), we have directly observed adatom motion between non-equivalent sites, dimer formation and dimer rotation. We found an influence of the dimers on the adatom motion, an influence of the adatoms on the dimer rotation and a mutual influence of the dimers on each other. The observed interactions have consequences for nucleation and thus growth. Our investigation suggests that it is important to understand diffusional properties and interaction of small adparticles beyond the adatom both experimentally and theoretically. We hope to stimulate theoretical work to understand why the influence of dimers on adatom motion is much more long-ranged than the similar influence of adatoms on adatom motion. We suggest to prepare surfaces predominantly with dimers to investigate this influence in more detail.

References

[1] Naumovets A G and Vedula Y S 1985 *Surf. Sci. Rep.* **4** 365
Bowker M and King D A 1978 *Surf. Sci.* **71** 583
Chumak A A and Tarasenko A A 1980 *Surf. Sci.* **91** 694
Reed S A and Ehrlich G 1981 *Surf. Sci.* **102** 588
Reed S A and Ehrlich G 1981 *Surf. Sci.* **105** 603
[2] Wang S C and Ehrlich G 1990 *Surf. Sci.* **239** 301
[3] Chen C L and Tsong T T 1990 *Phys. Rev.* B **41** 12403
[4] Gomer R 1990 *Rep. Prog. Phys.* **53** 917
[5] Kellog G L 1994 *Surf. Sci. Rep.* **21** 88
[6] Tringides M C (ed) 1997 *Surface Diffusion: Atomistic and Collective Processes* (New York: Plenum)
[7] Brune H 1998 *Surf. Sci. Rep.* **31** 121
[8] Ehrlich G 1991 *Surf. Sci.* **246** 1
Kyuno K and Ehrlich G 2000 *Phys. Rev. Lett.* **84** 2658
Wang S C and Ehrlich G 2002 *Phys. Rev.* B **65** 121407–1
[9] Linderoth T R, Horch S, Petersen L, Helveg S, Schœnning M, Lægsgaard E, Stensgaard I and Besenbacher F 2000 *Phys. Rev.* B **61** R2448
Linderoth T R, Horch S, Lægsgaard E, Stensgaard I and Besenbacher F 1998 *Surf. Sci.* **402** 308
[10] Mitsui T, Rose M K, Formin E, Ogletree D F and Salmeron M 2002 *Science* **297** 1850
[11] Wen J-M, Chang S-L, Burnett J W, Evans J W and Thiel P A 1994 *Phys. Rev. Lett.* **73** 2591
Wen J-M, Evans J W, Bartelt M C, Burnett J W and Thiel P A 1996 *Phys. Rev. Lett.* **76** 652
Cadilhe A M, Stoldt C R, Jenks C J, Thiel P A and Evans J W 2000 *Phys. Rev.* B **61** 4910

Morgenstern K, Rosenfeld G, Poelsema B and Comsa G 1995 *Phys. Rev. Lett.* **74** 2058
Morgenstern K, Rosenfeld G and Comsa G 1996 *Phys. Rev. Lett.* **76** 2113
Pai W W, Swan A K, Zhang Z and Wendelken J F 1997 *Phys. Rev. Lett.* **79** 3210
Eßer M, Morgenstern K, Rosenfeld G and Comsa G 1998 *Surf. Sci.* **402–404** 341
Morgenstern K, Rosenfeld G, Lægsgaard E, Besenbacher F and Comsa G 1998 *Phys. Rev. Lett.* **80** 556
Morgenstern K, Rosenfeld G and Comsa G 1999 *Surf. Sci.* **441** 289
Schlößer D C, Morgenstern K, Verheij L K, Rosenfeld G, Besenbacher F and Comsa G 2000 *Surf. Sci.* **465** 19
Morgenstern K, Lægsgaard E and Besenbacher F 2001 *Phys. Rev. Lett.* **86** 5739
[12] Boisvert Gh and Lewis L J 1999 *Phys. Rev.* B **59** 9846
[13] Vladimirova M, De Vita A and Pimpinelli A 2001 *Phys. Rev.* B **64** 245420–1
[14] Feenstra R M, Slavin A J, Held G A and Lutz M A 1991 *Phys. Rev. Lett.* **66** 3257
Kitamura S, Sato T and Iwatsuki M 1991 *Nature* **351** 215
Ganz E, Theiss S K, Hwang I S and Golovchenko J 1992 *Phys. Rev. Lett.* **68** 1567
Hwang I S, Theiss S K and Golovchenko J 1994 *Science* **265** 490
Mo Y W 1992 *Phys. Rev. Lett.* **69** 3643
Mo Y W 1993 *Phys. Rev. Lett.* **71** 2923
Kitamura N, Lagally M G and Webb M B 1993 *Phys. Rev. Lett.* **71** 2082
Zhang Z, Wu F, Zandvliet H J W, Poelsema B, Metiu H and Lagally M G 1995 *Phys. Rev. Lett.* **74** 3644
Linderoth T R, Horch S, Lægsgaard E, Stensgaard I and Besenbacher F 1997 *Phys. Rev. Lett.* **78** 4978
Linderoth T R, Horch S, Petersen L, Helveg S, Lægsgaard E, Stensgaard I and Besenbacher F 1999 *Phys. Rev. Lett.* **82** 1494
[15] Repp J, Moresco F, Meyer G, Rieder K-H, Hyldgaard P and Persson M 2000 *Phys. Rev. Lett.* **85** 2981
[16] Knorr N, Brune H, Epple M, Hirstein A, Schneider M A and Kern K 2002 *Phys. Rev.* B **65** 115420
[17] Repp J, Meyer G, Rieder K-H and Hyldgaard P 2003 *Phys. Rev. Lett.* **91** 206102
[18] Morgenstern K, Braun K-F and Rieder K H 2004 *Phys. Rev. Lett.* **93** 056102
[19] Morgenstern K 2005 *Phys. Status Solidi* b **242** 773
[20] Bogicevic A, Hyldgaard P, Wahnström G and Lundqvist B I 1998 *Phys. Rev. Lett.* **81** 172
[21] Bogicevic A 1999 *Phys. Rev. Lett.* **82** 5301
[22] Bogicevic A, Ovesson S, Hyldgaard P, Lundqvist B I, Brune H and Jennison D R 2000 *Phys. Rev. Lett.* **85** 1910
[23] Hyldgaard P and Persson M 2000 *J. Phys.: Condens. Matter* **12** L13
[24] Venables J A and Brune H 2002 *Phys. Rev.* B **66** 195404
[25] Silly F, Pivetta M, Ternes M, Patthey F, Pelz J P and Schneider W-D 2004 *Phys. Rev. Lett.* **92** 016101
[26] Braun K-F 2001 *PhD Thesis* Freie Universität Berlin
[27] Morgenstern K, Rosenfeld G, Poelsema B and Comsa G 1995 *Phys. Rev. Lett.* **74** 2058
[28] http://www.fkp.uni-hannover.de/∼morgenstern/
[29] Hofer W A, Garcia-Lekue A and Brune H 2004 *Chem. Phys. Lett.* **397** 354